

Superconductivity due to massless boson exchange in the strong-coupling limit

Andrey V. Chubukov¹ and Jörg Schmalian²

¹*Department of Physics and Condensed Matter Theory Center, University of Maryland, College Park, Maryland 20742, USA*

²*Department of Physics and Astronomy and Ames Laboratory, Iowa State University, Ames, Iowa 50011, USA*

(Received 24 July 2005; revised manuscript received 15 September 2005; published 29 November 2005)

We solve the problem of fermionic pairing mediated by a massless boson in the limit of large coupling constant. At weak coupling, the transition temperature is exponentially small and superconductivity is robust against phase fluctuation. In the strong coupling limit, the pair formation occurs at a temperature of the order of the Fermi energy, however, the actual transition temperature is much smaller due to phase and amplitude fluctuations of the pairing gap. Our model calculations describe superconductivity due to color magnetic interactions in quark matter and in systems close to a ferromagnetic quantum critical point with Ising symmetry. Our strong-coupling results are, however, more general and can be applied to other systems as well, including the antiferromagnetic exchange in 2D used for description of the cuprates.

DOI: [10.1103/PhysRevB.72.174520](https://doi.org/10.1103/PhysRevB.72.174520)

PACS number(s): 74.20.Mn, 71.10.Li

I. INTRODUCTION

Strong-coupling superconductivity due to the interaction between electrons and lattice vibrations has been successfully studied using the coupled Eliashberg equations¹ for the frequency-dependent normal and anomalous self-energies of superconductors.^{2–4} The theory finds its justification in the weakness of the corrections to the electron-phonon vertex, caused by the small ratio of the electron and ion masses.⁵ This theory inspired numerous efforts to describe superconductivity caused by other bosons,^{6–16} even though its justification turns out to be considerably more subtle in some of those cases.^{17–19} Important progress has been made in the study of pairing due to the exchange of bosons that are collective excitations of the fermions.^{6–16} In this context, the interplay between superconductivity and quantum criticality is particularly interesting^{20–26} as superconductivity in correlated electron systems often occurs in the proximity of a quantum critical point (QCP).^{27–31} At a QCP, the pairing boson becomes massless, and new and unexpected behavior emerges.^{20,25,32} A related problem occurs in the theory of quantum chromodynamics at high density where single-gluon exchange becomes dominant.³³ The exchange of gluons is believed to cause color superconductivity.^{34–36} As was pointed out by Son,³² and later in Refs. 37 and 38, the color magnetic interaction in high density QCD is unscreened at low temperatures, i.e., the pairing is mediated by a gapless boson. The pairing problem then becomes formally very similar to superconductivity at a QCP, even though the transition temperatures may be different by a factor of as big as 10^{12} .

In previous studies of the pairing problem near a QCP, the authors of Refs. 20, 25, and 32 assumed that the effective, boson-mediated fermion-fermion interaction u is much smaller than the fermionic bandwidth W (which is generally of the same order as E_F), i.e.,

$$g \sim \frac{u}{W} \ll 1. \quad (1)$$

The limit $g \ll 1$ is often called weak coupling. This notation is not quite correct, as near a QCP the smallness of g does

not imply that the system behaves as a weakly coupled Fermi liquid—the mass renormalization due to the exchange of a gapless boson is still singular in $D \leq 3$ and destroys the Fermi-liquid behavior at the QCP (see below). To simplify the notations, we nevertheless refer to $g \ll 1$ as weak coupling and $g \gg 1$ as strong coupling. With this notation the Eliashberg theory for superconductivity due to electron-phonon interaction^{2–4} is in the “weak-coupling” limit since $g \propto (v_s/v_F)\lambda$ is small. This is due to the smallness of the ratio v_s/v_F of the sound and Fermi velocities, while the product $\lambda = \rho_F V_{ep}$ of the electron-phonon interaction V_{ep} and the density of states at the Fermi level ρ_F can be of order unity.

The condition $g \ll 1$ implies that the pairing comes only from fermions in a tiny range of momenta around the Fermi surface, i.e., that the system behavior at energies comparable to E_F is irrelevant for the pairing. This makes the pairing problem universal and allows one to use well-established computational techniques, e.g., the Eliashberg theory.¹ However, for various systems of interest the interaction is not necessarily small. In particular, the same interaction that leads to the pairing is often also responsible for the onset of order at the QCP. Generic density-wave instabilities come from fermions with energies $O(E_F)$ and require g to be of order unity.³⁹ In the cuprate superconductors, to which the ideas of collective-mode mediated d -wave pairing was applied,^{15,16,24} the Hubbard interaction U is at least comparable to W as is evidenced by, e.g., the Heisenberg antiferromagnetism at half filling. For color superconductivity, the effective coupling u is also not necessarily small compared to E_F , and g well may be larger than 1.

These arguments call for an understanding of the pairing problem beyond the “weak-coupling” limit. In the present paper we extend previous “weak-coupling” studies of the pairing mediated by a gapless boson to the truly strong coupling limit $g \gg 1$. For definiteness we consider pairing of 3D electrons mediated by a scalar boson which is gapless at $q = 0$. This model describes p -wave superconductivity near a ferromagnetic Ising QCP, and color superconductivity of quarks. However, the results at strong coupling are quite general and can be applied to other systems as well, including

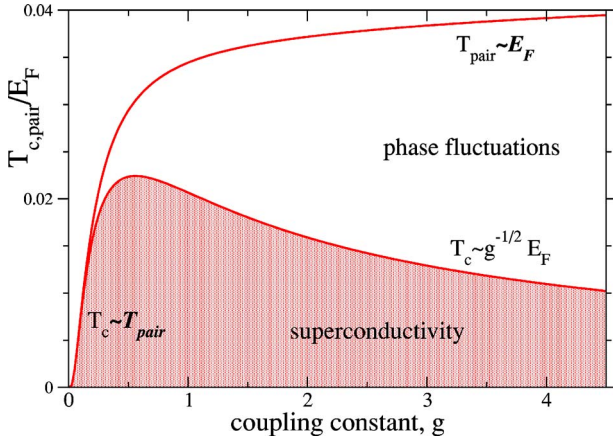


FIG. 1. (Color online) Schematic phase diagram for the superconducting transition temperature T_c and the pairing instability temperature T_{pair} as function of the dimensionless coupling constant g . While $T_c \approx T_{\text{pair}}$ for weak coupling, an intermediate regime $T_c < T_{\text{pair}}$ with phase (and amplitude) fluctuations occurs in the strong-coupling limit.

the antiferromagnetic exchange in 2D used for description of the cuprates. We discuss applications to other systems in a separate section. There is also a connection between our model and the interaction between conduction electrons, mediated by transverse photons.^{40,41} However, as shown in, Ref. 41, the exchange of transverse photons does not lead to superconductivity.

A word of caution: In the context of quark pairing mediated by gluons, the equation for the pairing vertex has only been derived in a gauge invariant manner at weak coupling.⁴² At strong coupling, antiparticle pairing, neglected in our model, may come into play. Still, qualitatively, the results obtained assuming only particle pairing likely remain valid at both weak and strong coupling.

The main results of this paper are summarized in the phase diagram, Fig. 1. In the weak-coupling limit, we find, in agreement with Son³² and others,^{37,38} that the transition temperature behaves, to leading exponential order, as

$$\ln \frac{\omega_0}{T_c} = \frac{\pi}{2\sqrt{g}}, \quad (2)$$

where $\omega_0 \sim E_F/g$. This result is parametrically larger than the usual BCS result⁴³ $\ln \omega_0/T_c \propto 1/g$, and the difference is due to the gapless nature of the pairing boson (see below). Still, T_c is exponentially small at small g .

At $g = O(1)$, T_c becomes of order E_F , although the prefactor for T_c is a small number. At even larger g , we find two characteristic temperatures. The larger temperature T_{pair} sets the onset of pairing, and is of order E_F (again, with a small prefactor). The smaller temperature, T_c is of order $\sqrt{\omega_0 E_F} \sim E_F/\sqrt{g} \ll E_F$. This temperature is determined by the superfluid stiffness, and sets the scale for phase coherence, i.e., of the actual superconductivity. In between $T_c \sim E_F/\sqrt{g}$ and $T_{\text{pair}} \sim E_F$, the system displays pseudogap behavior: pairs of fermions are already formed, but do not move coherently.

The accuracy of the computations is a central issue for the theoretical analysis near a QCP. At small g , one can use Eliashberg theory since the relevant bosonic and fermionic frequencies are much smaller than E_F . Although the frequency-dependent self-energy (included in our theory) is not small due to the fact that the near criticality, vertex corrections, and the momentum-dependent self-energy (not included in our theory) are exponentially small (see below). At $g = O(1)$, typical frequencies become of order E_F , vertex corrections become $O(1)$, and the momentum-dependent self-energy becomes of the same order as the frequency-dependent self-energy. In this situation, no reliable theoretical scheme is possible.

A naive expectation would be that at strong coupling, vertex corrections get even stronger. We show, however, that at larger g , vertex corrections actually saturate at a value $O(1)$ and do not grow with g . At the same time, the momentum-dependent term in the self-energy again becomes small compared to its frequency dependence, this time the relative smallness is in $1/g$. Furthermore, the pairing problem at $g \gg 1$ still involves fermions with energies below E_F for which the density of states can be approximated by a constant. As a result, this version of the Eliashberg theory (more accurately, the local theory) becomes qualitatively valid. This local theory is different from the original Eliashberg theory in that the lattice cannot be neglected, and the existence of a finite bosonic bandwidth now plays a crucial role. Still, as in the Eliashberg theory, we derive closed-form equations for the fermionic self-energy and the pairing vertex. To justify the local approximation at $g > 1$ quantitatively, we extend the model to N fermion flavors and consider the limit of large N .²⁴ In this case, vertex corrections become of order $1/N$ and can be safely neglected.

The structure of the paper is as follows. In the next section we set up the model and define the large N limit used to perform the strong coupling calculation. In Sec. III we briefly discuss the weak coupling limit and present an alternative derivation of Son's result³² for T_c . In Sec. IV we solve the pairing problem at strong coupling. In Sec. V we analyze gap fluctuations and demonstrate the existence of two characteristic temperature scales. In Sec. VI we justify our computational procedure. In Sec. VII we discuss other systems, including the cuprates. The last section presents our conclusions. Several technical details are presented in the Appendixes.

II. MODEL AND LARGE N EXPANSION

We consider the pairing problem in which 3D fermions ψ_k interact via exchanging a massless, bosonic mode with a static propagator $D_q^{(0)} = 1/q^2$:

$$\mathcal{H}_{\text{int}} = - \sum_q \frac{u(q)}{k_F} D_q^{(0)} \sum_{k,k'} \psi_{k+q}^\dagger \psi_{k'-q}^\dagger \psi_{k'} \psi_k. \quad (3)$$

Here k_F is the Fermi momentum, and $u(q) > 0$ is the effective interaction (with the dimension of energy), which decays at typical $q \sim k_F$. Another energy scale in the problem is the fermionic bandwidth W [roughly, the scale up to which the

fermionic dispersion ε_k can be linearized around Fermi surface $\varepsilon_k = v_F(k - k_F)$. The ratio of the two characteristic energies defines the dimensionless coupling constant g in Eq. (1). The interaction (3) may actually be in the spin channel, as for a ferromagnetic problem, but for simplicity we drop spin indices. Still, the overall sign in Eq. (3) is attractive, i.e., is opposite to that in systems with Coulomb interaction.²⁶ Also for simplicity we model $u(q)$ by a step function $u(q) = u\theta(q_0 - q)$, where $q_0 \leq k_F$. We then restrict all momentum integrals to $q < q_0$. The interaction (3) leads to pairing, and also gives rise to fermionic and bosonic self-energies $\Sigma_k(\omega)$ and $\Pi_q(\Omega)$, respectively. The two self-energies are related to fermionic and bosonic propagators via

$$G_k^{-1}(\omega) = i\omega - v_F(k - k_F) - \Sigma_k(\omega),$$

$$D_q^{-1}(\Omega) = q^2 + \Pi_q(\Omega). \quad (4)$$

In order to perform a controlled calculation at strong coupling, we generalize the model of Eq. (4) to N fermion flavors and rescale $v_F \rightarrow Nv_F$ and $u \rightarrow Nu$. In what follows, we assume that the new v_F and u are constants, independent of N . The details of this large- N approach are summarized in Appendix A.

The generalized Eliashberg theory is a set of three coupled integral equations for the pairing vertex Φ and the self-energies Σ and Π . As we assumed $u(q)$ to be constant at small q , Φ does not depend on momentum, i.e., the equation for Φ is formally the same as for s -wave pairing. This does not imply, though, that the actual pairing is s wave. In particular, for a ferromagnetic case, the spin structure of the interaction implies that the pairing is in the p channel and Φ is the amplitude of a momentum-dependent pairing function.

We will primarily be interested in the onset of the pairing and consider the linearized equation for Φ , and normal state expressions for Σ and Π . Then the system of three coupled equations has the form

$$\Phi(\omega) = \frac{u}{k_F} \int_{q, \omega'} D_q(\omega - \omega') \Phi(\omega') G_{k_F+q}(\omega') G_{k_F+q}(-\omega'),$$

$$\Sigma(\omega) = \frac{u}{k_F} \int_{q, \omega'} D_q(\omega - \omega') G_{k_F+q}(\omega'),$$

$$\Pi_q(\Omega) = \frac{u}{k_F} \int_{k, \omega} G_k(\omega) G_{k+q}(\omega + \Omega). \quad (5)$$

We used the notation $\int_{q, \omega} \dots = \int [d^3q / (2\pi)^3] T \sum_{\omega_n} \dots$ with Matsubara frequencies $\Omega_n = 2n\pi T$ and $\omega_n = (2n+1)\pi T$ for bosons and fermions, respectively.

Equations (5) neglect vertex corrections and the momentum dependence of Σ and Φ . We will argue below that at large N , both approximations hold both at weak and at strong coupling. Physically, these approximations are based on the (verifiable) assumption that bosons are slow modes compared to fermions. This allows one to factorize the momentum integration in Eqs. (5). Namely, for every given \mathbf{k}_F along the Fermi surface, the integration over the component q_\perp transverse to Fermi surface in the equations for Φ and Σ

involves only fast fermions, while integrating over the remaining two momentum components q_\parallel in the bosonic propagator, one can set $q_\perp = 0$. This implies that the boson propagator actually only appears in Eqs. (5) through the ‘‘local’’ interaction (see Appendix A):

$$d(\Omega) = \int_0^{q_0} q_\parallel dq_\parallel D_{q_\parallel, q_\perp=0}(\Omega), \quad (6)$$

where $q_0 \sim k_F$ is the upper cutoff in the integral over q_\parallel . As a result, the equations for Φ and Σ in Eq. (5) reduce to

$$\Phi(\omega) = \frac{3g}{2} \int d\omega' \frac{\Phi(\omega') d(\omega - \omega')}{|\omega' + i\Sigma(\omega')|},$$

$$\Sigma(\omega) = -i \frac{3g}{2} \int d\Omega \operatorname{sgn}(\Omega + \omega) d(\Omega), \quad (7)$$

where the factor of $\frac{3}{2}$ is for further convenience and the coupling constant g is given as

$$g = \frac{u}{24\pi^2 E_F^*}, \quad (8)$$

with $E_F^* = v_F k_F / 2$. Without approximation we can explicitly solve for $\Pi(\Omega)$ and find²⁴

$$\Pi(q, \Omega) = \gamma \frac{|\Omega|}{q}, \quad (9)$$

where

$$\gamma = 12\pi^2 k_F^3 \frac{g}{E_F^*}. \quad (10)$$

Note that γ does not depend on N , despite the fact that the Landau damping term contains a flavor index N as an overall factor. Details of the derivation of Eqs. (7) and (9) are given in Appendix A.

For the ‘‘local’’ interaction (6), we obtain from Eqs. (4) and (9):

$$d(\Omega) = \frac{1}{3} \ln \left(1 + \frac{\omega_0}{|\Omega|} \right), \quad (11)$$

where ω_0 is the characteristic frequency of the bosonic degrees of freedom:

$$\omega_0 = \frac{q_0^3}{\gamma} = \frac{E_F}{g} \quad (12)$$

and we introduced

$$E_F = \frac{E_F^*}{12} \left(\frac{q_0}{\pi k_F} \right)^3. \quad (13)$$

Below we will refer to E_F as to Fermi energy. We should keep in mind however that our E_F depends on the choice of the upper momentum cutoff q_0 and is only of the same order of magnitude as an actual Fermi energy of the system (it can actually be much smaller than Fermi energy if the interaction is dominated by near-forward scattering, and $q_0 \ll k_F$).

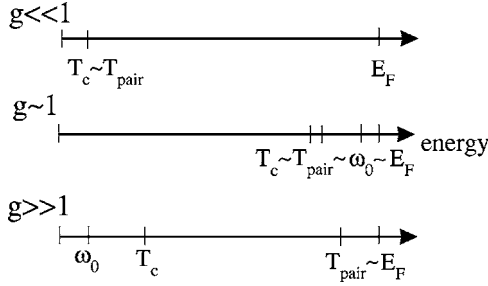


FIG. 2. Characteristic energy scales for the weak- ($g \ll 1$), intermediate- ($g \sim 1$), and strong- ($g \gg 1$) coupling limit. While at weak coupling, $\omega_0 \approx E_F/g$ is large compared to E_F and thus irrelevant, it emerges as a new low-energy scale in the strong coupling limit.

Substituting Eq. (11) into Eq. (5) and integrating over frequency, we obtain

$$i\Sigma(\omega) = \omega g \left(\frac{\omega_0}{|\omega|} \ln \frac{\omega_0 + |\omega|}{\omega_0} + \ln \frac{\omega_0 + |\omega|}{|\omega|} \right) = \begin{cases} \omega g \ln \frac{\omega_0}{|\omega|}, & |\omega| \ll \omega_0, \\ \text{sgn}(\omega) g \omega_0 \ln \frac{|\omega|}{\omega_0}, & |\omega| \gg \omega_0. \end{cases} \quad (14)$$

We see that ω_0 sets the scale at which the momentum cutoff in the bosonic propagator begins affecting the fermionic self-energy. At low energies, the cutoff is irrelevant, and the self-energy has the form typical for a marginal Fermi liquid.⁴⁴ At $\omega > \omega_0$, the self-energy almost saturates and only logarithmically depends on frequency. At weak coupling, $\omega_0 = E_F/g > E_F$, and the crossover is meaningless as Eq. (14) only holds up to $\omega \sim E_F$ [we recall that in obtaining Eq. (14) we approximated the density of states by a constant]. The marginal Fermi liquid behavior then extends all the way up to E_F . At strong coupling $\omega_0 \ll E_F$, and the crossover in $\Sigma(\omega)$ occurs well below E_F . In this situation, marginal Fermi-liquid behavior only holds at small frequencies $\omega < E_F/g$, while at $E_F/g < \omega < E_F$, $\Sigma(\omega)$ depends logarithmically on frequency (see Fig. 2).

The crossover in the self-energy at strong coupling parallels the crossover in the “local” bosonic propagator $d(\omega)$ in Eq. (11)

$$d(\Omega) = \begin{cases} \frac{1}{3} \ln \frac{\omega_0}{|\Omega|}, & |\Omega| \ll \omega_0, \\ \frac{1}{3} \frac{\omega_0}{|\Omega|}, & |\Omega| \gg \omega_0. \end{cases} \quad (15)$$

As for the self-energy, this crossover is meaningful only at strong coupling, when $\omega_0 < E_F$.

Substituting the self-energy and $d(\Omega)$ into the equation for the pairing vertex, we obtain

$$\Phi(\omega) = \frac{g}{2} \int d\omega' \frac{\Phi(\omega')}{|\omega' + i\Sigma(\omega')|} \ln \left(1 + \frac{\omega_0}{|\omega - \omega'|} \right). \quad (16)$$

Strictly speaking, we have to evaluate this equation at finite T , because the linearized equation for Φ is only valid at the onset temperature for the pairing. For reasons that we outline below, we label this temperature as T_{pair} rather than T_c . As we will only be interested in the order of magnitude estimate for T_{pair} , we adopt a simplified approach, and instead of performing the discrete Matsubara sum, use Eq. (16) at finite T , but introduce a lower frequency cutoff at $\omega \sim T$. In the weak coupling limit, this procedure was shown earlier³⁸ to yield the same T_{pair} (modulo a numerical prefactor), as one would obtain by performing an explicit summation over discrete Matsubara frequencies. In Appendix C we show that the same holds for large g . With this simplification we have to solve

$$\Phi(\omega) = g \int_{T_{\text{pair}}}^{\infty} d\omega' \frac{\Phi(\omega')}{|\omega' + i\Sigma(\omega')|} K(\omega, \omega'), \quad (17)$$

with bosonic kernel

$$K(\omega, \omega') = \frac{1}{2} \ln \left[\left(1 + \frac{\omega_0}{|\omega - \omega'|} \right) \left(1 + \frac{\omega_0}{|\omega + \omega'|} \right) \right]. \quad (18)$$

In what follows we solve this equation, first in the weak coupling limit $g \ll 1$, where we reproduce the results of Ref. 32, and then in the strong-coupling limit $g \gg 1$.

III. PAIRING PROBLEM AT WEAK COUPLING

At weak coupling, one obviously expects T_{pair} to be much smaller than ω_0 (see Fig. 2). This in turn implies that only frequencies $\omega \ll \omega_0$ are relevant. For these frequencies, the self-energy $\Sigma(\omega)$ and the kernel $K(\omega, \omega')$ in Eq. (18) can be simplified to

$$\Sigma(\omega) = -i\omega g \ln \frac{\omega_0}{|\omega|},$$

$$K(\omega, \omega') = \ln \frac{\omega_0}{\sqrt{|\omega^2 - \omega'^2|}}. \quad (19)$$

Equation (17) then becomes

$$\Phi(\omega) = g \int_{T_{\text{pair}}}^{\omega_0} d\omega' \frac{\Phi(\omega') \ln \frac{\omega_0}{\sqrt{|\omega^2 - \omega'^2|}}}{\omega' \left(1 + g \omega' \ln \frac{\omega_0}{\omega'} \right)}. \quad (20)$$

This equation yields T_{pair} for the pairing in a marginal Fermi liquid. Equation (20) was solved numerically in Ref. 45. We show that an analytic solution is also possible. Our computational procedure is similar to the one used by Son.³² In addition to the approach of Ref. 32 we also analyze the pairing susceptibility.

If the two logarithmic terms in the right-hand side (RHS) of Eq. (20) were absent, the equation for the pairing vertex would be the same as in BCS theory,⁴³ and T_{pair} would scale

as $\omega_0 e^{-1/g}$. However, as Son demonstrated,³² the presence of the logarithm in the pairing kernel substantially enhances T_{pair} at weak coupling and changes its functional form to $T_{\text{pair}} \propto \omega_0 e^{-\pi/(2\sqrt{g})}$. The easiest way to see this is to introduce logarithmic variables $x = \ln(\omega_0/\omega)$, $x' = \ln(\omega_0/\omega')$, $x_T = \ln(\omega_0/T)$, and rewrite Eq. (20) with logarithmic accuracy as

$$\Phi(x) = g \int_0^x dx' \frac{x' \Phi(x')}{1 + gx'} + gx \int_x^{x_T} dx' \frac{\Phi(x')}{1 + gx'}. \quad (21)$$

Differentiating both sides of Eq. (21) over x , we find

$$\frac{d\Phi(x)}{dx} = g \int_x^{x_T} \frac{\Phi(x')}{1 + gx'}. \quad (22)$$

Differentiating one more time, we find that the integral equation for the anomalous vertex reduces to a second-order differential equation

$$\frac{d^2\Phi(x)}{dx^2} = -g \frac{\Phi(x)}{1 + gx}. \quad (23)$$

The gx term on the RHS of Eq. (23) is due to the fermionic self-energy. We assume and verify afterwards that $gx \ll 1$ for all relevant x , and drop this term from Eq. (23). The solution of Eq. (23) is then elementary:

$$\Phi(x) = A \cos(\sqrt{gx}) + B \sin(\sqrt{gx}). \quad (24)$$

The two boundary conditions

$$\begin{aligned} \Phi(x=0) &= 0, \\ \left. \frac{d\Phi(x)}{dx} \right|_{x=x_T} &= 0 \end{aligned} \quad (25)$$

follow from Eqs. (21) and (22), respectively. They yield $A=0$, and

$$\cos(\sqrt{gx_T}) = 0. \quad (26)$$

The onset temperature T_{pair} corresponds to the smallest x_T that satisfies Eq. (26), i.e., to $x_T \sqrt{g} = \pi/2$. Ignoring pre-exponential factors, we then reproduce Son's result³²

$$T_{\text{pair}} \approx \omega_0 e^{-\pi/2\sqrt{g}}. \quad (27)$$

The relevant value of x are $x_T \propto 1/\sqrt{g}$, i.e., $gx \sim gx_T \sim \sqrt{g} \ll 1$. This justifies dropping the gx term (i.e., fermionic self-energy) from Eq. (23). The first-order correction to T_{pair} due to the self-energy was analyzed in Ref. 46 in the context of color superconductivity.

To get more insight into the pairing instability, it is also instructive to analyze the pairing susceptibility $\chi_{pp}(\omega, T)$. This is done by adding an infinitesimally small external pairing field Φ_0 to the RHS of Eq. (20).⁴⁷ The pairing susceptibility is

$$\chi_{pp}(\omega, T) = \left. \frac{\partial \Phi(\omega, T)}{\partial \Phi_0} \right|_{\Phi_0 \rightarrow 0} = \frac{\Phi(\omega, T)}{\Phi_0}.$$

At $T > T_{\text{pair}}$, $\Phi(\omega) \propto \Phi_0$, and the pairing susceptibility is finite. If the transition is of second order, $\chi_{pp}(\omega, T)$ diverges

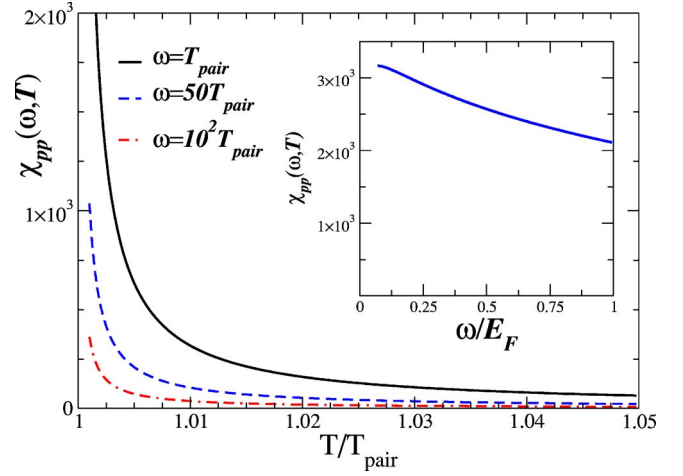


FIG. 3. (Color online) Particle-particle response function $\chi_{pp}(\omega, T)$ for $g=0.1$ as function of T for various energies. Inset: $\chi_{pp}(\omega, T)$ as a function of energy for $T=1.001T_c$.

at T_{pair} . In BCS theory, $\Phi(\omega, T)$ does not depend on frequency, and $\chi_{pp}(\omega, T) = 1/g \log(T/T_{\text{pair}})$. This pairing susceptibility is obviously positive above T_{pair} , diverges at T_{pair} for all ω , and is negative below T_{pair} , implying that the normal state is unstable against pairing. In our case χ_{pp} can easily be obtained from the solution of Eq. (23) by changing the boundary condition at $x=0$ to $\Phi(x=0) = \Phi_0$. We then obtain $\Phi(x)$ given by Eq. (24) with

$$A = \Phi_0, \quad B = \Phi_0 \tan(\sqrt{gx_T}) \quad (28)$$

and

$$\chi_{pp}(\omega, T) = \frac{\cos\left(\sqrt{g} \ln \frac{\omega}{T}\right)}{\cos\left(\sqrt{g} \ln \frac{\omega_0}{T}\right)}. \quad (29)$$

Note that T and ω_0 are lower and upper limits of the integration over ω in Eq. (20), hence the pairing susceptibility is only defined in the interval $T < \omega < \omega_0$. We see from Eq. (29) that at the upper boundary, $\omega = \omega_0$, $\chi_{pp} = 1$ at any T . This is a clear distinction to the BCS limit. As long as $T > T_{\text{pair}}$, the pairing susceptibility remains positive everywhere in the interval $T < \omega < \omega_0$ despite the fact that the solution of the differential equation (23) for $\Phi(\omega)$ is formally an oscillating function of frequency. At T_{pair} , $\ln(\omega_0/T) = \pi/2\sqrt{g}$, and χ_{pp} diverges for all ω , except $\omega = \omega_0$. Below T_{pair} , χ_{pp} is negative at low frequencies, implying that the system is unstable towards pairing. We show the behavior of $\chi_{pp}(\omega, T)$ as function of temperature and frequency in Fig. 3.

IV. PAIRING PROBLEM AT STRONG COUPLING

We next analyze the strong coupling limit $g \gg 1$. In distinction to the weak-coupling regime, we now have two characteristic energy scales in the problem, $\omega_0 = E_F/g \ll E_F$, and E_F , which is the ultimate upper cutoff in the theory (see Fig. 2). The issue then is which of the two scales determines the onset of the pairing.

Suppose momentarily that only frequencies $\omega \leq \omega_0$ contribute to the pairing. At $\omega < \omega_0$, the pairing kernel and the self-energy can still be approximated by Eq. (19), and the equation for the pairing vertex can still be reduced to the differential equation (23). In distinction to the weak-coupling case, however, the term gx , coming from the self-energy, is now the dominant term in the denominator on the RHS of Eq. (23). Leaving only this term, we arrive at

$$\frac{d^2\Phi(x)}{dx^2} = -\frac{\Phi(x)}{x}. \quad (30)$$

Note that g drops from this equation because of cancellation between g factors in the effective interaction and the self-energy.

The solution of Eq. (23) with $\Phi(x=0)=0$ is $\Phi(x) \propto \sqrt{x}J_1(2\sqrt{x})$, where J_1 is a Bessel function. Substituting this solution back into Eq. (21) and assuming that the upper limit in the frequency integral in Eq. (21) is still x_T (i.e., that only $\omega < \omega_0$ are relevant for the pairing), we obtain $x_T=3.670(5)$. This leads to $T_{\text{pair}} \approx 0.025\omega_0$, i.e., to a pairing instability at a temperature which is a fraction of ω_0 .

This result is similar to McMillan's $T_{\text{pair}} \sim \omega_D e^{-(1+g)/g} \sim \omega_D$ for strongly coupled phonon superconductors³ (ω_D is Debye frequency). However, as for phonons, there is actually no reason to restrict the frequency integral to $\omega < \omega_0 \sim E_F/g$, since for strong coupling there also exists a wide frequency range $\omega_0 < \omega < E_F$ where, on the one hand, the pairing kernel and the self-energy are different from Eq. (19), and, on the other hand, typical frequencies are still below E_F , i.e., a low-energy description is at least qualitatively valid. The existence of this extra range raises the possibility that the onset of pairing may occur at a temperature of order E_F , not of order $\omega_0 \sim E_F/g$. Note that for the electron-phonon case, the scale which sets the ultimate upper cutoff for the pairing (the analog of E_F in our case) is $\omega_D \sqrt{g}$.⁴⁸⁻⁵¹

To verify whether T_{pair} scales as E_F , not as ω_0 , we analyze the equation for $\Phi(\omega)$ assuming that all characteristic frequencies are larger than ω_0 . At these frequencies, the pairing kernel and the self-energy are given by

$$\begin{aligned} \Sigma(\omega) &= -i \operatorname{sgn}(\omega) g \omega_0 \ln \frac{|\omega|}{\omega_0}, \\ K(\omega, \omega') &= \frac{\omega_0}{2} \left(\frac{1}{|\omega - \omega'|} + \frac{1}{|\omega + \omega'|} \right). \end{aligned} \quad (31)$$

Now the pairing kernel scales as $1/\omega$, while the self-energy is nearly a constant, and only logarithmically depends on frequency.

Substituting the pairing kernel and the self-energy into Eq. (17) and using the fact that for all $\omega < E_F$ the self-energy $\Sigma(\omega)$ exceeds the bare ω , we obtain

$$\Phi(\omega) = \int_T^{E_F} \frac{d\omega' \Phi(\omega')}{2 \ln \frac{\omega'}{\omega_0}} \left(\frac{1}{|\omega - \omega'|} + \frac{1}{|\omega + \omega'|} \right). \quad (32)$$

The logarithmic divergence on the RHS of Eq. (32) at $\omega = \omega'$ can easily be regularized as the $1/|\omega - \omega'|$ form of the kernel is only valid at $|\omega - \omega'| > \omega_0$.

We see that the dimensionless ratio T/E_F is the only parameter in Eq. (32), except for the $\ln(\omega'/\omega_0)$ term in the denominator in Eq. (32). Hence, if this equation has a solution at some finite value of this parameter, the pairing instability should occur at $T \sim E_F$.

The analysis of Eq. (32) requires special care because of the interplay between the $1/\omega$ dependence of the pairing kernel and logarithmic behavior of the self-energy. The discussion is somewhat technical, and we moved it into Appendix B. We find there that the solution of Eq. (32) at frequencies between T and E_F is

$$\Phi(\omega) = A \frac{E_F}{\sqrt{\omega}} \cos \left[\beta \ln \frac{\omega}{E_F} + \phi \right], \quad (33)$$

where $\beta=0.7923(2)$ is determined from the solution of a transcendental equation, and A, ϕ are real constants.

As at weak coupling, the two limits of the integration over ω' in Eq. (32) for Φ imply two boundary conditions for $\Phi(\omega)$ from Eq. (33). One of them determines the phase ϕ , while the other determines the pairing instability temperature [the overall factor A in Eq. (33) cannot be determined from the linearized gap equation]. For a simple estimate of T_{pair} , we use the same boundary conditions as in the weak coupling limit, i.e., (i) assume that frequencies larger than E_F are irrelevant for the pairing and set $\Phi(\omega=E_F)=0$ and (ii) assume that $d\Phi(\omega)/d\omega|_{\omega=T_{\text{pair}}}=0$. We then obtain $\phi=\pi/2$ and

$$T_{\text{pair}} = E_F e^{-1/\beta^*} \approx 0.0676 E_F, \quad (34)$$

where $1/\beta^* = (1/\beta) \arccos(-1/\sqrt{1+4\beta^2}) \approx 1/0.371$. In Appendix C we demonstrate that the same result, modulo a numerical prefactor, is obtained by solving explicitly the linearized gap equation for discrete Matsubara frequencies.

We see therefore that at strong coupling, the pairing instability temperature T_{pair} is indeed of the order of the Fermi energy E_F , although numerically it is still much smaller than E_F . This temperature is larger by a factor g than the McMillan-type estimate $T_{\text{pair}} \approx \omega_0$, which ignores the pairing interaction at energies larger than the characteristic bosonic frequency. We emphasize that in order to obtain Eq. (34), it was crucial that we included into consideration the normal-state self-energy renormalization. Had we ignored it, an oscillating solution for $\Phi(\omega)$ at $\omega > \omega_0$ would not have been possible, i.e., no pairing instability would occur at $T > \omega_0$ (see Ref. 38). Alternatively speaking, $T_{\text{pair}} \sim E_F$ is the result of the interplay between a non-Fermi-liquid behavior of the fermions caused by the logarithmic self-energy $\Sigma(\omega) \propto g \omega_0 \ln(|\omega|/\omega_0)$, and a retarded pairing interaction governed by a "local" boson susceptibility $d(\omega) \propto 1/\omega$.

Since $T_{\text{pair}} \sim E_F$, it is inevitable that the magnitude of T_{pair} is affected by the system behavior at high energies, i.e., at lattice scales in the condensed matter context. We assumed above that the fermionic density of states is a constant. This is indeed only approximately valid at $\omega \sim E_F$. To determine T_{pair} beyond an order of magnitude estimate, one then needs to solve the full microscopic problem. Still, lattice effects only modify the prefactor in T_{pair} ; the relation $T_{\text{pair}} \sim E_F$ is generic and survives lattice corrections.

V. THE ROLE OF GAP FLUCTUATIONS

A. Phase fluctuations

In the weak-coupling limit it is known that the transition temperature, determined from the linearized gap equation, coincides with the temperature where global phase coherency sets in. This can easily be seen by evaluating the phase stiffness ρ_s defined as

$$E_{\text{phase}} = \rho_s \int d^3x (\nabla\varphi)^2. \quad (35)$$

At weak coupling, $\rho_s \approx E_F k_F$. Equation (35) can then be considered as the continuum limit of an XY -spin model on a three-dimensional lattice with lattice constant $\approx k_F^{-1}$ and exchange interaction $\approx E_F$. Fluctuation effects in this model become effective at temperatures comparable to the exchange interaction, i.e., at temperatures comparable to the Fermi energy. Since $T_{\text{pair}} \ll E_F$, fluctuations at $T \sim T_{\text{pair}}$ are ineffective, and phase coherency is established as soon as Cooper pairs are formed, i.e., $T_{\text{pair}} = T_c$.

Consider next the strong-coupling limit, where $T_{\text{pair}} \sim E_F$. In what follows we argue that at strong coupling, $\rho_s/k_F \approx E_F/\sqrt{g} \ll T_{\text{pair}}$. In this situation, phase fluctuations become relevant well below the onset of the pairing, and by conventional reasoning,⁵²⁻⁵⁴ phase coherence sets in at

$$T_c \approx E_F/\sqrt{g} \ll T_{\text{pair}} \approx E_F. \quad (36)$$

This new energy scale is the characteristic energy of a boson in the gapped state below T_{pair} . In between T_{pair} and T_c , the system displays a pseudogap behavior: the density of states develops a maximum at a finite frequency (the tunneling gap), and the spectral weight is transformed from frequencies below the gap to frequencies above the gap. However, the superconducting order parameter only develops at T_c .

We now show how we arrived at $\rho_s/k_F \approx E_F/\sqrt{g}$. The superfluid stiffness at $T=0$ is obtained by evaluating the sum of fermionic bubbles made of normal and anomalous Green's functions, and is given by

$$\rho_s = \rho_s^0 \int_0^\infty d\omega \frac{\Phi^2(\omega)}{\{[\omega Z(\omega)]^2 + \Phi^2(\omega)\}^{3/2}}, \quad (37)$$

where $\rho_s^0 \sim E_F k_F$ is the stiffness of a BCS superconductor. $\Phi(\omega)$ is the pairing vertex at $T=0$ and we introduced

$$Z(\omega) = 1 - \frac{\Sigma(\omega)}{i\omega}. \quad (38)$$

Using the relation between $\Phi(\omega)$ and the gap function $\Delta(\omega) = \Phi(\omega)/Z(\omega)$, one can write Eq. (37) as

$$\rho_s = \rho_s^0 \int_0^\infty \frac{d\omega}{Z(\omega)} \frac{\Delta^2(\omega)}{[\omega^2 + \Delta^2(\omega)]^{3/2}}. \quad (39)$$

For a BCS superconductor, $Z=1$, and Δ does not depend on frequency. The frequency integration in Eq. (39) then yields $\rho_s = \rho_s^0$, independent on Δ . This essentially implies that at $T=0$, the superfluid density equals the full density.

To obtain ρ_s at strong coupling, we need to know $\Delta(\omega, T=0)$ and $Z(\omega, T=0)$. The gap $\Delta(\omega, T=0) = \Delta(\omega)$ is obtained by solving the nonlinear gap equation

$$\Delta(\omega) = \frac{3g}{2} \int_{-\infty}^\infty \frac{\left[\Delta(\omega') - \Delta(\omega) \frac{\omega'}{\omega} \right] d_{\text{sc}}(\omega - \omega')}{\sqrt{\omega'^2 + \Delta(\omega')^2}} d\omega', \quad (40)$$

where $d_{\text{sc}}(\Omega)$ is the ‘‘local’’ boson propagator in a superconductor. In the normal state, $d(\Omega)$ is given by Eqs. (11) and (15). In the presence of Δ , the bosonic spectrum itself changes due to feedback from the gap opening, and the Landau damping transforms into $\Pi(\Omega) \sim \gamma(\Omega^2/q\Delta) \approx \gamma(\Omega^2/qE_F)$ (Ref. 24). This leads to

$$d_{\text{sc}}(\Omega) = \frac{1}{3} \ln \left(1 + \frac{\omega_{0,\text{sc}}^2}{\Omega^2} \right), \quad (41)$$

where

$$\omega_{0,\text{sc}} \sim \sqrt{\omega_0 E_F} \sim E_F/\sqrt{g} \quad (42)$$

is the characteristic energy of the bosons in a state where fermions are gapped—it has the same physical meaning as ω_0 above T_{pair} . For frequencies $E_F > |\Omega| > \omega_{0,\text{sc}}$ we have

$$d_{\text{sc}}(\Omega) \approx \frac{1}{3} \left(\frac{\omega_{0,\text{sc}}}{\Omega} \right)^2. \quad (43)$$

Despite the $1/\Omega^2$ dependence of $d_{\text{sc}}(\Omega)$, the integral over ω' in Eq. (40) remains convergent since the numerator vanishes at $\omega = \omega'$. We can then safely use Eq. (43) for $d_{\text{sc}}(\Omega)$ and drop the restriction that this form is only valid above $\omega_{0,\text{sc}}$. The gap equation then contains only E_F as the energy scale. Accordingly, $\Delta(\omega)$ can only be of order E_F , if the gap equation indeed has a solution. We verified that the solution of Eq. (43) does indeed exist and yields $\Delta(\omega) = E_F f(\omega/E_F)$.

The expression for $Z(\omega)$ follows from the formula for the self-energy

$$Z(\omega) = 1 + \frac{3g}{2\omega} \int_{-\infty}^\infty \frac{d(\omega - \omega') \omega' d\omega'}{\sqrt{\omega'^2 + \Delta(\omega')^2}}. \quad (44)$$

Here the restriction that Eq. (43) is only valid at frequencies above $\omega_{0,\text{sc}}$ becomes crucial, otherwise the integral over ω' in Eq. (44) would diverge. Beyond this, the evaluation of the integral is straightforward, and we obtain

$$Z(\omega < E_F) \approx g^{1/2}, \quad Z(\omega \geq E_F) \approx 1. \quad (45)$$

Substituting this Z into Eq. (39), we find

$$\rho_s(T=0) \approx \rho_s^0 / \sqrt{g} \approx \omega_{0,sc} k_F. \quad (46)$$

We see that $\rho_s(T=0)/k_F$ is much smaller than T_{pair} . The exchange constant of the XY model (35) is therefore $\omega_{0,sc} \ll E_F$. This leads to our estimate of T_c in Eq. (36). This estimate is further supported by the fact that a finite T , we found that the leading temperature dependence of the stiffness varies as a function of $T/\omega_{0,sc}$, i.e., thermal corrections to the stiffness indeed become relevant at $T \approx \omega_{0,sc}$.

B. The role of the screening

In the above consideration we assumed that the boson that causes pairing and superconductivity remain massless below T_{pair} , i.e., the effective interaction remains long ranged. Then one immediately is confronted with the question whether screening effects lead to a finite range of the interaction, i.e. whether the boson acquires a mass large enough to change the physical conclusions of our theory. The issue of screening has to be discussed separately for high density quarks pairing by gluons and for the pairing near a (magnetic) quantum-critical point.

The gluons are gauge bosons and acquire a mass only via a Higgs mechanism in the superconducting state. In other words, the mass appears due to a feedback from the pairing on the pairing boson. At weak coupling, the role of screening was considered in Ref. 32, where it was shown that these screening does not change Eq. (27) for $T_c \approx T_{\text{pair}}$. At strong coupling, the situation is more subtle as we have to consider the behavior below T_{pair} , in order to determine the actual transition temperature T_c . Redoing the calculation that led to the local boson propagator in Eq. (41), but now assuming that because of screening, q^2 is replaced by $q^2 + m^2$, we find that a finite mass m will not change Eq. (36) for T_c if the relevant frequencies obey

$$\Omega > \omega_{0,sc} \left(\frac{m}{k_F} \right)^2.$$

Since typical $\Omega \gg \omega_{0,sc}$, the condition $m < k_F$ is sufficient to ensure that screening is irrelevant. An upper bound for m can be obtained by evaluating the polarization bubble at $q=0$ in the superconducting state. A calculation very similar to the one that led to ρ_s , Eq. (46) yields that $m^2 \approx k_F^2 g^{-1/2}$, i.e., for large g , $m \ll k_F$, and hence screening effects do not change our results, even as $T_c \ll T_{\text{pair}}$.

For the pairing near a QCP, the situation is similar. The only exception is that now the bosonic propagator does contain a mass which vanishes at the QCP. The actual mass includes fluctuation effects, i.e., the correction from $\Pi_{q=0}(0)$ even in the normal state: $m^2 = m_0^2 + \Pi_{q=0}(\omega=0)$, where m_0 is a bare mass. Still, the renormalized mass m vanishes at the QCP and hence T_{pair} is correctly obtained using a massless boson. Within an RPA theory, the condition $m=0$ coincides with the Stoner criterion. Below T_{pair} , an extra mass is generated by the feedback from the pairing state. However, as in the case discussed above, this does not affect our results for T_c in both weak- and strong-coupling limits [but it may for intermediate coupling, where all corrections are $O(1)$].

C. A relation to Eliashberg theory

We emphasized above that our strong-coupling theory is a local theory, but not an Eliashberg theory. Indeed, in our case, the interaction is larger than the Fermi energy, and the presence of the momentum cutoff in the bosonic propagator is crucial. This distinction becomes particularly important if we compare our result for ρ_s with the conventional Eliashberg theory. There E_F is the *largest* scale in the problem, even if the “local” interaction $d(\omega)$ scales as $1/\omega$ or even faster (as, e.g., $1/\omega^2$ for phonon superconductors). Once E_F is the largest energy scale, ρ_s/k_F is always larger than T_{pair} , and phase fluctuations are weak. Indeed, according to Eq. (37), ρ_s scales as

$$\rho_s \sim \rho_s^0 \frac{\Delta}{\Sigma(\omega \sim \Delta)}, \quad (47)$$

where, as before, $\rho_s^0 \sim E_F k_F$ is the stiffness of the weak-coupling limit. The ratio Δ/Σ can be quite small if the pairing occurs in the quantum-critical regime and involves near-massless bosons. In particular, for phonon superconductors, when the Debye frequency ω_D is much smaller than electron-phonon interaction u , $\Delta \sim T_{\text{pair}} \sim u$ (see Ref. 48), and $\Sigma(\omega \sim u) \sim u^2/\omega_D \gg \Delta$. Then $\rho_s \sim \rho_s^0(\omega_D/u) \ll \rho_s^0$. Still, the condition that E_F is the largest energy scale implies that $\Sigma(\omega) < E_F$, i.e., $u^2/\omega_D < E_F$. Then, even though ρ_s is reduced from its weak-coupling value, it still holds that

$$\rho_s/k_F \sim T_{\text{pair}} \frac{E_F \omega_D}{u^2} > T_{\text{pair}}. \quad (48)$$

This implies that the exchange coupling in the corresponding XY model is still larger than the onset temperature for the pairing. As a result, within Eliashberg theory one can expect at most modest changes in the transition temperature due to phase fluctuations. In our case, we remind, at strong coupling E_F is no longer the largest energy scale in the problem, and the $1/\omega$ form of $d(\omega)$ in the strong-coupling limit emerges once one imposes a cutoff in the integration over bosonic momenta.

D. Longitudinal gap fluctuations

In previous subsections we discussed the role of phase fluctuations. They are sufficient to destroy superconducting order between T_c and T_{pair} . There also exist, however, longitudinal fluctuations of the pairing gap, and it is instructive to consider how strong they are.

Longitudinal gap fluctuations generally reflect how shallow the profile of the free energy with respect to deviations of $\Delta(\omega)$ from its equilibrium value is. A shallow profile implies that the superconducting order is weak as different $\Delta(\omega)$ have almost the same condensation energy. A situation with a shallow profile emerges when, in real frequencies, the attractive part of $\text{Re } d_{sc}(\omega)$ is weak, and the pairing predominantly comes from $\text{Im } d_{sc}(\omega)$. The imaginary part of a “local” interaction describes purely retarded interaction between fermions. This interaction then does not contribute to the superconducting order parameter, which is an equal time correlator. Accordingly, the slope of the free energy is determined only by a weak $\text{Re } d_{sc}(\omega)$.

A simple estimate of the energy scale at which longitudinal gap fluctuations become relevant can be obtained by analyzing the form of $\text{Re } d_{\text{sc}}(\omega)$. Converting Eq. (41) to real frequencies yields

$$d_{\text{sc}}(\Omega) = \frac{1}{3} \ln \left(\left| 1 - \frac{\omega_{0,\text{sc}}^2}{\Omega^2} \right| \right) + i \frac{\pi \text{sgn } \Omega}{3} \theta(\Omega^2 - \omega_{0,\text{sc}}^2). \quad (49)$$

We see that $\text{Re } d_{\text{sc}}(\omega)$ remains attractive up to a frequency $\omega_{0,\text{sc}}/\sqrt{2}$, and is repulsive at larger frequencies. This means that frequencies above $\omega_{0,\text{sc}}/\sqrt{2}$ do not contribute to the superconducting order parameter, although they do contribute to the pairing itself via $\text{Im } d_{\text{sc}}(\omega)$. This in turn implies that longitudinal gap fluctuations become strong at $T \geq \omega_{0,\text{sc}} \sim E_F/\sqrt{g}$. Comparing this result with Eq. (36), we see that in our strong-coupling limit, phase and amplitude fluctuations of the gap are equally important, as the corrections to the superconducting order parameter from both fluctuations become $O(1)$ at $T \sim T_c \sim E_F/\sqrt{g}$. One can equally argue that $T_c \ll T_{\text{pair}}$ is the result of strong phase fluctuations, or the result of soft longitudinal gap fluctuations brought about by the absence of a repulsive component of $\text{Re } d_{\text{sc}}(\omega)$ at $\Omega > \omega_{0,\text{sc}}$.

VI. MIGDAL PARAMETER

As we discussed in the Introduction, the coupled equations (5) for the pairing vertex and fermionic and bosonic self-energies are valid if vertex corrections and the momentum-dependent part of the self-energy can be neglected. In case of electron-phonon interaction, this approximation was justified by Migdal.⁵ Below we evaluate the leading corrections to our local theory, both in the Eliashberg limit, and at strong coupling. For definiteness, we focus on vertex corrections $\delta\Gamma$ of the total vertex

$$\Gamma = \sqrt{\frac{u}{k_F}} (1 + \delta\Gamma).$$

Generally, the correction to the interaction vertex between fermions and gapless bosons, depend on the interplay between the bosonic momentum and frequency. In particular, Ward identities imply that vertex corrections in the limit of vanishing bosonic momentum are of the same order as the fermionic self-energy, and not necessary small.⁵⁵ However, for the pairing problem, we need to analyze vertex corrections for typical bosonic energies Ω_{typ} and for typical bosonic momenta q_{typ} that contribute to the pairing.

The leading vertex correction in the normal state is presented in Fig. 4 and is given by

$$\delta\Gamma_q(\omega, \Omega) = \frac{Nu}{k_F} \int_{k', \omega'} D_{k-k'}(\omega - \omega') G_{k'}(\omega') G_{k'+q}(\omega' + \Omega). \quad (50)$$

Here, ω is the external fermionic frequency. In principle, $\delta\Gamma$ depends on two momenta—the bosonic momentum q and the external fermionic momentum k . However, the dependence

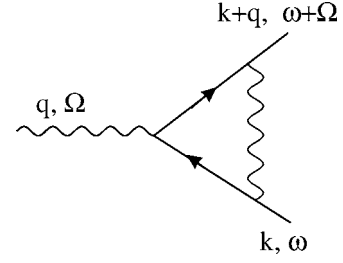


FIG. 4. Leading correction of the fermion boson vertex $\Gamma_{k,q}(\omega, \Omega)$. The solid lines stand for the fermionic propagator and the wiggly lines for the bosonic propagator, respectively.

on k is weak and thus irrelevant, and we will neglect it. Performing the momentum integration in Eq. (50), we obtain

$$\delta\Gamma_q(\omega, \Omega) \approx \frac{3g \int_0^\Omega d(\omega + \omega') d\omega'}{\sqrt{\Omega^2 + (Nv_Fq)^2}}. \quad (51)$$

The factor N in the denominator is a consequence of the rescaling that we performed in Sec. II. In the limit $q \rightarrow 0$

$$\delta\Gamma_{q \rightarrow 0}(\omega, \Omega) = \frac{3g}{\Omega} \int_\omega^{\Omega+\omega} d(\omega') d\omega' = \frac{\Sigma(\Omega + \omega) - \Sigma(\omega)}{-i\Omega}. \quad (52)$$

This is the Ward identity relating the homogeneous vertex with the self-energy. We see from Eq. (52) that static vertex corrections do not depend on N and are not small at moderate and strong coupling. The situation, however, changes when we evaluate $\delta\Gamma_q(\omega, \Omega)$ at q_{typ} and Ω_{typ} relevant to the pairing problem. In what follows we evaluate $\delta\Gamma$ for weak, intermediate and strong coupling, and specify in each case the relevant bosonic momentum and frequency.

A. Vertex corrections at weak coupling

We first consider the limit of weak coupling $g \ll 1$. The typical bosonic energy Ω_{typ} is of order $T_c \approx (E_F/g)e^{-\pi/(2\sqrt{g})}$. On the other hand, typical momenta q_{typ} are obtained from the condition that the momentum and frequency dependent term in the bosonic propagator $D(q, \Omega)$ are of the same order, i.e., $q_{\text{typ}} \approx (\gamma\Omega_{\text{typ}})^{1/3}$. Together with Eq. (10) for γ this yields

$$v_F q_{\text{typ}} \approx E_F e^{-\pi/(6\sqrt{g})}. \quad (53)$$

Comparing Ω and $v_F q$, we see that

$$v_F q_{\text{typ}} \approx \Omega_{\text{typ}} [g e^{\pi/(3\sqrt{g})}] \gg \Omega_{\text{typ}}. \quad (54)$$

We then obtain from Eq. (51)

$$\delta\Gamma \approx \frac{g \int_0^{\Omega_{\text{typ}}} \ln\left(\frac{\omega_0}{\omega}\right) d\omega'}{Nv_F q_{\text{typ}}} = \frac{\pi}{2N} \frac{e^{-\pi/3\sqrt{g}}}{\sqrt{g}}. \quad (55)$$

We see that vertex correction is exponentially small for small g . The extension to large N is in fact not needed as vertex corrections are already negligible.

B. Vertex corrections at intermediate coupling

At intermediate $g=O(1)$, ω_0 and E_F become of the same order, i.e., there is only one characteristic energy scale in the problem. Vertex corrections are $O(1)$ for $N=1$, but are still small in $1/N$ if we extend the theory to large N .

C. Vertex corrections at strong coupling

A naive expectation would be that vertex corrections gradually increase with g and eventually overcome the overall smallness in $1/N$. This would invalidate our local theory at sufficiently large g . It turns out, however, that vertex corrections freeze at $O(1/N)$ and do not grow with g . The saturation originates from the form of the bosonic propagator $D(q, \Omega)$, which is determined by the self-energy $\approx \gamma(|\Omega|/q)$. As γ by itself scales with the boson-fermion coupling, $D(q, \omega)$ scales inversely with g and cancels out the overall factor g in Eq. (51).

To see this explicitly we note that at strong coupling, q_{typ} is of order k_F , hence $v_F q_{\text{typ}}$ is of order E_F . Typical frequencies Ω_{typ} are also $O(E_F)$. The external fermionic frequency ω in Eq. (51) is also of order of the Fermi energy. Evaluating the vertex correction diagram using $d(\Omega) \approx \omega_0/3|\Omega|$, we obtain for these q_{typ} and Ω_{typ}

$$\delta\Gamma \approx \frac{g \int_0^{E_F} \frac{\omega_0}{E_F + \omega'} d\omega'}{E_F \sqrt{1+N^2}} \approx \frac{1}{N}. \quad (56)$$

We see that vertex corrections indeed do not depend on g and remain small (at large N) for arbitrary strong coupling. At large N , vertex corrections remain small for all values of g , i.e., our local theory is valid both in the weak- and the strong-coupling limit.

VII. OTHER SYSTEMS

As discussed in the Introduction, the problem discussed in this paper describes p -wave superconductivity in condensed matter systems close to a ferromagnetic quantum critical point with Ising symmetry,⁵⁶ and superconductivity due to color magnetic interactions in dense quark matter.^{32,37,38} As pointed out above, for color superconductivity, antiparticle pairing that has been neglected in Eqs. (5) and (7), may come into play at strong coupling.⁴² We nevertheless believe that the main results of this paper are still relevant to this case.

However, the results obtained in the strong-coupling limit are much more general and in fact do not require quantum criticality. The key aspect of our theory is that the boson propagator $D_q(\Omega)$ becomes completely local above a certain frequency, even if momenta are of order $q_0 \leq k_F$. We considered a particular case when boson dynamics is set by Landau damping, and

$$d(\Omega) \propto \frac{\omega_0}{|\Omega|}, \quad (57)$$

where ω_0 is a characteristic upper cutoff scale of the boson system. However, our results will be equally valid for any $d(\Omega)$ in the form $d(\Omega) \propto 1/|\Omega|^\gamma$ with $\gamma \geq 1$.

To make a connection to other studies of electron pairing at strong coupling, we note that at $q \sim q_0 \sim k_F$, our pairing interaction behaves as $(u/k_F^3)/(1+A|\Omega|)$, where $A \sim u/(E_F^*)^2$. Meanwhile, in Hubbard-type models, the pairing interaction mediated by either spin or charge fluctuations behaves, at a generic $q \sim k_F$, as $(U^2/tk_F^3)/(1+\bar{A}|\Omega|)$ where $\bar{A} \sim (U/E_F^*)^2/t$, and U and t are the local interaction and tight binding hopping element, respectively. In obtaining the effective interaction, we assumed that the static pairing interaction has an RPA form $U^2\chi_0(q)/[1-U\chi_0(q)]$, and for a generic $q \sim k_F$, $U^2\chi_0(q) \sim U^2/t \leq 1$. Comparing the two forms of the interaction, we find $u \sim U^2/t$.

We first note that our strong-coupling results are in agreement with the studies of the attractive Hubbard model at $U \gg t$.⁶⁶ Indeed, in our case $g=(U/t)^2$, $\omega_0 \sim E_F/g \propto t^3/U^2$, and $\omega_{0,s} \sim E_F/\sqrt{g} \sim t^2/U \sim J$, where $J \sim t^2/U$ is a short-range magnetic interaction between electrons. Hence $T_{\text{pair}} \sim \Delta \sim t$, while $T_c \sim J \ll T_{\text{pair}}$.

Another application of our strong-coupling result is d -wave pairing by antiferromagnetic fluctuations in 2D, which has been discussed in great detail in the context of cuprate superconductors.²⁴ That analysis was, however, performed within the low-energy spin-fermion model, which is only valid at $u < E_F$, i.e., in the weak-coupling limit, as we defined it in this paper. In the cuprates, as is well known, the Hubbard interaction is comparable to E_F , i.e., $g \geq 1$. Our finding that a large pseudogap regime with phase incoherent pairs is inevitable at strong coupling is quite intriguing in view of numerous observations of pseudogap physics in this class of materials.

The extension of our results to d -wave pairing requires some extra justification as once we neglect the momentum dependence of the pairing kernel, we must make sure that we do not lose the d -wave component of the pairing gap. One way to proceed is to assume, as we did before in applying our results to a ferromagnetic case, that the interaction is momentum independent over some range of q with the width q_0 , and vanishes elsewhere. For the antiferromagnetic case, this range is centered around $q_1=(\pi/a, \pi/a)$, although this does not matter much if $q_0 \sim k_F \sim 1/a$ (a is interatomic spacing). The extension of Eq. (13) to 2D cuprates then yields $T_{\text{ins}} \sim t$ and $T_c \sim \rho_s \sim J$. This agrees with numerical investigations of variational wave functions designed to cover the strong-coupling limit.⁵⁷ These studies do indeed yield a zero temperature gap $\Delta \sim t$ and a considerably reduced $T_c \sim \rho_s \sim J$.⁵⁸⁻⁶⁰

Alternatively, one could use the quantum-critical approach as in Ref. 24 and assume that the interaction $u(q)$ is a constant (i.e., not a step function), and that the static $D(q)$ has an Ornstein-Zernike form near q_1 : $D(q) \propto [\xi^{-2} + (q - q_1)^2]^{-1}$. In this situation, the momentum dependence of the interaction cannot be neglected, even at very large frequencies, as otherwise one would not obtain a d -wave component of the pairing kernel. Applying the same reasoning as in the preceding sections we then obtain that at strong coupling $g \gg 1$, frequencies larger than ω_0 do not contribute to the pairing, and both T_{pair} and T_c scale with ω_0 , although T_c is smaller numerically because of both phase and longitudinal gap fluctuations. Within this line of reasoning, the pairing

comes from momenta near (π, π) , for which $U\chi_0(\pi, \pi) \approx 1$, hence $u \sim U^2\chi_0(\pi) \sim U$. Substituting this into $\omega_0 \sim E_F^2/u$, we obtain $\omega_0 \sim J^{61-63}$

Which of the two model momentum dependences is better is unclear as no detailed information is available yet about the behavior of the static spin susceptibility. The physics that we described in this paper is more prominent if the effective interaction is strongly momentum dependent and is closer to a step function. We note, however, that in both cases, $T_c = O(J)$, while the momentum dependence of the effective interaction only affects the width of the temperature range between T_c and T_{pair} .

There also exists some similarity between our results and those obtained for the crossover from BCS-type behavior at weak coupling and Bose Einstein condensation (BEC) of pairs at strong coupling.⁶⁴⁻⁶⁷ In particular, for large g , when Δ is of order E_F , our pair coherence length $\xi \approx v_F/\Delta$ becomes of the order of the typical distance between fermions ($\sim k_F^{-1}$). This is similar to the findings for the BCS-BEC crossover.^{64,65,67} An important distinction between the two theories is that in BCS-BEC crossover, the pairing interaction is static, while in our case it is dynamic and strongly retarded. The transition at large g in our case should therefore not be considered as condensation of almost free bosons.

VIII. CONCLUSION

In this paper we considered pairing of 3D fermions, due to an exchange of massless bosons. The model we considered describes superconductivity in itinerant fermionic systems close to a ferromagnetic quantum critical point with Ising symmetry, and superconductivity due to color magnetic interactions in quark matter.

At weak coupling, we find that an exchange of a massless boson enhances T_c compared to the BCS expectation $T_c^{\text{BCS}} \propto e^{-1/g}$, and the actual transition temperature is $T_c \approx \omega_0 e^{-\pi/2\sqrt{g}}$, where $\omega_0 = E_F/g$ is a characteristic energy scale of the bosons. This result agrees with previous calculations.^{32,37,38}

At strong coupling, we find that pairing emerges at a temperature $T_{\text{pair}} \approx 0.06E_F$, which is only numerically smaller than the Fermi energy. In addition, we find that the phase stiffness behaves as $\rho_s \sim T_{\text{pair}}/\sqrt{g}$, i.e., the typical energy scale where phase fluctuation, become important is parametrically smaller than T_{pair} . The small phase stiffness implies that coherent superconductivity only emerges at $T_c \approx T_{\text{pair}}/\sqrt{g} \ll T_{\text{pair}}$. In between T_c and T_{pair} the system displays pseudogap behavior with preformed pairs. The width of the pseudogap regime widens as g grows.

We further argued that several aspects of the strong-coupling solution, particularly the existence of two temperatures T_{pair} and T_c , are valid for a much larger class of problems in which boson propagator becomes completely local above a certain frequency. The existence of a cutoff energy scale, which corresponds to the finite lattice constant in the condensed matter context or to the large density in case of color superconductivity, is crucial for the relevance of phase fluctuations.

Note added in proofs. For an interesting related study of strong coupling effects in superconductors, see Ref. 69.

ACKNOWLEDGMENTS

This work was supported in part by the National Science Foundation Grant Nos. NSF DMR02-40238 (A.C.) and PHY99-07949 and by the Ames Laboratory, operated for the U.S. Department of Energy by Iowa State University under Contract No. W-7405-Eng-82 (J.S.). Part of this work was carried out when both of us participated in the 2005 workshop on ‘‘Quantum phase transitions’’ at the Kavli Institute for Theoretical Physics. We acknowledge useful conversations with M. Dzero, P. Coleman, V. Khodel, D. Maslov, C. Pepin, and V. Yakovenko.

APPENDIX A: DETAILS OF THE LARGE- N APPROACH

In this appendix we discuss the details of the large- N approach, where N is the number of fermionic flavors. We demonstrate how one obtains Eqs. (7) in $N \rightarrow \infty$ limit. In a different, but related context, the large- N theory was presented in Ref. 24.

In order to have a well defined $N \rightarrow \infty$ limit, an extension to large N usually requires an appropriate rescaling of the parameters in the Hamiltonian. In what follows, we demonstrate that the rescaling $v_F \rightarrow v_F N$ and $u \rightarrow uN$ yields the desired behavior. Physically, this rescaling is appropriate for a situation where the bosons are slow modes compared to fermions.

We first evaluate explicitly $\Sigma_k(\omega)$ and $\Pi_q(\Omega)$ from Eq. (5) and demonstrate that $N \rightarrow \infty$ limit yields nontrivial zeroth order results for both fermionic and bosonic self-energies. For the fermionic self-energy at the Fermi surface ($k = k_F$), we have

$$\Sigma(\omega) = \frac{Nu}{k_F(4\pi)^4} \int \frac{D_q(\omega')d\omega'd^3q}{i(\tilde{\omega}' + \tilde{\omega}) - v_F N q_{\perp}}. \quad (\text{A1})$$

Here $\tilde{\omega} = \omega + \Sigma(\omega)$ includes self-energy renormalization of an intermediate fermion, and q_{\perp} is the component of the fermionic momentum perpendicular to the Fermi surface. Substituting $\varepsilon = v_F N q_{\perp}$ yields

$$\Sigma(\omega) = \frac{u}{v_F k_F (4\pi)^4} \int \frac{D_q(\omega')d\omega'd^2q_{\parallel}d\varepsilon}{i(\tilde{\omega}' + \tilde{\omega}) - \varepsilon}. \quad (\text{A2})$$

In the limit of large N it holds $q^2 = q_{\parallel}^2 + (\varepsilon/v_F N)^2 \approx q_{\parallel}^2$, i.e., $D_q(\omega') \approx D_{q_{\parallel}}(\omega')$ and the integrations over $d\varepsilon$ and d^2q_{\parallel} decouple. Introducing

$$d(\Omega) = \int_0^{q_0} q_{\parallel} dq_{\parallel} D_{q_{\parallel}}(\Omega) \quad (\text{A3})$$

as in Eq. (6), and using

$$\int_{-\infty}^{\infty} d\varepsilon \frac{1}{i\tilde{\omega} - \varepsilon} = -i\pi \text{sgn}(\omega), \quad (\text{A4})$$

we obtain $\Sigma(\omega)$ as in Eq. (7). A very similar calculation shows that $\Sigma_k(0) \propto (k - k_F)$ is of order $1/N$. In Sec. VI we

demonstrated that vertex corrections are also of order $1/N$.

Consider next the anomalous self-energy. We have

$$\Phi(\omega) = \frac{Nu}{k_F(2\pi)^4} \int \frac{D_q(\omega - \omega')\Phi(\omega')d^3q d\omega'}{\tilde{\omega}'^2 + (v_F N q_\perp)^2}. \quad (\text{A5})$$

Using the same substitution $\varepsilon = v_F N q_\perp$, we rewrite Eq. (A5) as

$$\Phi(\omega) = \frac{u}{v_F k_F (2\pi)^4} \int \frac{D_q(\omega - \omega')\Phi(\omega')d\omega' d^2q_\parallel d\varepsilon}{\tilde{\omega}'^2 + \varepsilon^2}. \quad (\text{A6})$$

For large N we again approximate D_q by D_{q_\parallel} , then the integrations over $d\varepsilon$ and d^2q_\parallel decouple again, and we obtain Eq. (5). We observe that the prefactor in Eq. (A6) is independent on N , i.e., the rescaling $v_F \rightarrow v_F N$ and $u \rightarrow uN$ guarantees that $\Xi(\omega)$ and $\Phi(\omega)$ are both nontrivial in the limit $N \rightarrow \infty$.

Consider next the bosonic propagator. We must keep in mind that a closed fermion loop yields a prefactor N in front of $\Pi_q(\Omega)$. We then evaluate

$$\Pi_q(\Omega) = N \frac{Nu}{k_F} \int_{k,\omega} G_k(\omega) G_{k+q}(\omega + \Omega). \quad (\text{A7})$$

Evaluating the integral, we find that N cancels out, and

$$\Pi_q(\Omega) = \gamma \frac{|\Omega|}{q} \quad (\text{A8})$$

with $\gamma = uk_F/2v_F^2$, as in Eq. (9). We emphasize that the cancellation of N occurs due to the presence of the additional flavor index N as an overall factor in Eq. (A7).

Consider now the generic structure of the Feynman diagrams for the thermodynamic potential. Each running fermionic line yields a factor $1/v_F$, i.e., after rescaling it contributes a factor $1/N$. Similarly, each diagram with $2n$ vertices scales as u^n and acquires a prefactor N^n after rescaling $u \rightarrow uN$. Finally, if a given diagram for the thermodynamic potential has m closed fermion loops, a summation over fermionic flavors yields an additional prefactor N^m . Since in a given diagram for the thermodynamic potential, the number of internal fermionic lines is the same as the number of vertices, it follows that a diagram with $2n$ vertices and m closed fermionic loops behaves as

$$\Xi \propto N^{m-n}. \quad (\text{A9})$$

The thermodynamic potential for the “zero-order” theory consists of rings of connected particle hole loops and bosonic lines, and has $m=n$, i.e., $\Xi_0 = O(1)$. The fermionic and bosonic self-energies are obtained from Ξ_0 by cutting one fermionic (or bosonic) line, and are also of order 1 as they indeed should be in the “zero-order” theory. Note, however, that this independence of N is the result of the interplay between u and v_F as if one cuts a fermionic line one loses one factor N since one closed fermionic loop disappears. This is compensated by the fact that there is one running fermionic line less in the diagram.

The diagrams which constitute the expansion in $1/N$ are then obtained by reducing the number of independent internal fermionic loops at a given number of u . The leading

corrections have $m=n-1$ and hence are of order $1/N$. One can make sure that these diagrams account for vertex corrections to the “zero-order” theory.

APPENDIX B: PAIRING WITH $1/|\omega - \omega'|$ KERNEL

In this appendix we obtain the solution of the Eliashberg equation, Eq. (32), in the strong-coupling regime. The analysis of a pairing problem with a kernel $1/|\omega - \omega'|$ is nontrivial and it is useful to solve a more general problem first.⁶⁸ We consider

$$h_\gamma(\omega) = \frac{1 - \gamma}{2} \int_0^\infty \frac{d\omega' h_\gamma(\omega') k_\gamma(\omega, \omega')}{(\omega')^{1-\gamma}} \quad (\text{B1})$$

with

$$k_\gamma(\omega, \omega') = \frac{1}{|\omega - \omega'|^\gamma} + \frac{1}{|\omega + \omega'|^\gamma} \quad (\text{B2})$$

and argue below that $\Phi(\omega) \simeq \lim_{\gamma \rightarrow 1} h_\gamma(\omega)$.

The integral equation (B1) is scale invariant suggesting a power-law solution

$$h_\gamma(\omega) = A\omega^{-b}. \quad (\text{B3})$$

Inserting this ansatz into Eq. (B1) we obtain

$$1 = \frac{1 - \gamma}{2} \int_0^\infty dt \frac{1}{t^{1+b-\gamma}} \left(\frac{1}{|t-1|^\gamma} + \frac{1}{|t+1|^\gamma} \right), \quad (\text{B4})$$

where $t = \omega'/\omega$. This determines the exponent $b(\gamma)$. The integral over t can be performed explicitly. In the limit where γ is close to 1, Eq. (B4) reduces to

$$1 = 1 + (1 - \gamma)y(b), \quad (\text{B5})$$

where $y(b) = \gamma_E + \psi(b) - (\pi/2)\tan(b\pi/2)$, and $\psi(b)$ is the digamma function. While b is undetermined for $\gamma=1$ it must hold that $y(b)=0$ for any $\gamma \neq 1$. For real b the condition $y(b)=0$ cannot be fulfilled. However, for a complex $b = \alpha + i\beta$, we find that the imaginary part of $y(b)$ vanishes if $\alpha = \frac{1}{2}$, i.e. if $y(\frac{1}{2} + i\beta)$ is purely real. Using this fact and substituting $b = 1/2 + i\beta$ into Eq. (B5), we obtain that β is determined from

$$\text{Re} \left[\gamma_E + \psi \left(\frac{1}{2} + i\beta \right) \right] = \frac{\pi}{2} \tan \left(\frac{\pi}{4} + i \frac{\pi\beta}{2} \right). \quad (\text{B6})$$

This equation is easily solved graphically and yields $\beta = \pm 0.7923(2)$. Therefore

$$h_\gamma(\omega) = A\omega^{-1/2-i\beta} + A^* \omega^{-1/2+i\beta}. \quad (\text{B7})$$

The overall constant A is chosen such that $h_\gamma(\omega)$ is real.

In order to show that Eq. (B7) is indeed the solution of Eq. (32) we discuss more carefully why $\lim_{\gamma \rightarrow 1} h_\gamma(\omega)$ gives the desired $\Phi(\omega)$. Equation (32) can be reexpressed as

$$\Phi(\omega) = \lim_{\gamma \rightarrow 1} \frac{1 - \gamma}{2} \int_T^{E_F} \frac{d\omega' \Phi(\omega') k_\gamma(\omega, \omega')}{\omega'^{1-\gamma} - \omega_0^{1-\gamma}}. \quad (\text{B8})$$

This equation coincides with Eq. (B1) if we neglect $\omega_0^{1-\gamma}$ in the denominator. We now recall that at strong coupling,

$T_{\text{pair}} \gg \omega_0$. Then for all $\omega' > T$ in Eq. (B8) holds that $\omega' \gg \omega_0$, and we can safely neglect $\omega_0^{1-\gamma}$ for any $\gamma \neq 1$.

APPENDIX C: LINEARIZED GAP EQUATION FOR DISCRETE MATSUBARA FREQUENCIES

In the computation of T_{pair} in the main text we imposed the lower cutoff in the zero-temperature equation for the pairing vertex. In the weak coupling limit, this procedure was shown earlier³⁸ to yield the same T_{pair} (modulo a numerical prefactor), as one would obtain by performing an explicit summation over discrete Matsubara frequencies. In this appendix we demonstrate that the same is true in the strong-coupling limit.

The most straightforward way to analyze the linearized pairing problem is by considering the gap function

$$\Delta_n = \frac{\Phi(\omega_n)}{Z(\omega_n)}, \quad (\text{C1})$$

where $Z(\omega_n) = 1 - \Sigma(\omega_n)/i\omega_n$ and determine the temperature at which $\Delta_n \neq 0$ for the first time. The advantage of analyzing Δ instead of Φ is that the corresponding linearized gap equation

does not explicitly contain the fermionic self-energy and can more easily be solved numerically. The equation for Δ_n is straightforwardly obtained from the equations for $\Phi(\omega_n)$ and $\Sigma(\omega_n)$:

$$\Delta_n = 3\pi g T \sum_m \left(\frac{\Delta_m}{\omega_m} - \frac{\Delta_n}{\omega_n} \right) \text{sgn}(\omega_m) d(\omega_m - \omega_n). \quad (\text{C2})$$

In the limit where $T_{\text{pair}} > \omega_0$, relevant $|\omega_n| > \omega_0$, we can approximate $d(\Omega_n)$ by $d(\Omega_n) \approx \omega_0/3|\Omega_n|$. Then

$$\Delta_n = \frac{E_F}{4\pi T_{\text{pair}}} \sum_{m \neq n} \left(\frac{\Delta_m}{m+1/2} - \frac{\Delta_n}{n+1/2} \right) \frac{\text{sgn}(m+1/2)}{|m-n|}. \quad (\text{C3})$$

The summation over discrete Matsubara frequencies is convergent for large n . Thus, no regularization or cut off is needed to solve for Δ_m . The only dimensionless parameter in Eq. (C3) is E_F/T_{pair} and the nontrivial solution of Eq. (C3), if it exists, appears at $T_{\text{pair}} \approx E_F$ as we found earlier. We verified numerically that the solution of Eq. (C3) does indeed exist at $T_{\text{pair}} \approx 0.064E_F$. This is even quantitatively close to the estimate $T_{\text{pair}} \approx 0.0676E_F$ obtained in the main text.

-
- ¹G. M. Eliashberg, Sov. Phys. JETP **11**, 696 (1960); **16**, 780 (1963).
²D. J. Scalapino, in *Superconductivity*, edited by R. D. Parks (Decker, New York, 1969), Vol. 1, p. 449.
³W. L. McMillan, Phys. Rev. **167**, 331 (1968).
⁴F. Marsiglio and J. P. Carbotte, in *The Physics of Superconductors*, edited by K. H. Bennemann and J. B. Ketterson (Springer, Berlin, 2003), Vol. 1.
⁵A. Migdal, Sov. Phys. JETP **7**, 996 (1958).
⁶V. J. Emery, Ann. Phys. (N.Y.) **28**, 1 (1964).
⁷N. F. Berk and J. R. Schrieffer, Phys. Rev. Lett. **17**, 433 (1966).
⁸P. W. Anderson and R. F. Brinkman, Phys. Rev. Lett. **30**, 1108 (1973).
⁹P. W. Anderson and P. Morel, Phys. Rev. **123**, 1911 (1961).
¹⁰A. J. Leggett, Rev. Mod. Phys. **47**, 331 (1975).
¹¹V. J. Emery, Synth. Met. **13**, 21 (1986).
¹²K. Miyake, S. Schmitt-Rink, and C. M. Varma, Phys. Rev. B **34**, 6554 (1986).
¹³D. J. Scalapino, E. Loh, Jr., and J. E. Hirsch, Phys. Rev. B **34**, 8190 (1986).
¹⁴P. Monthoux, A. V. Balatsky, and D. Pines, Phys. Rev. Lett. **67**, 3448 (1991).
¹⁵D. J. Scalapino, Phys. Rep. **250**, 329 (1995).
¹⁶P. Monthoux and D. Pines, Phys. Rev. Lett. **69**, 961 (1992). D. Pines, Z. Phys. B: Condens. Matter **103**, 129 (1997).
¹⁷J. R. Schrieffer, J. Low Temp. Phys. **99**, 397 (1995).
¹⁸A. V. Chubukov, Phys. Rev. B **52**, R3840 (1995).
¹⁹B. L. Altshuler, L. B. Ioffe, and A. J. Millis, Phys. Rev. B **52**, 5563 (1995).
²⁰Ar. Abanov, A. Chubukov, and A. Finkel'stein, Europhys. Lett. **54**, 488 (2001).
²¹R. Roussev and A. J. Millis, Phys. Rev. B **63**, 140504(R) (2001).
²²Z. Wang, W. Mao, and K. Bedell, Phys. Rev. Lett. **87**, 257001 (2001).
²³M. Dzero and L. P. Gor'kov, Phys. Rev. B **69**, 092501 (2004).
²⁴A. Abanov, A. V. Chubukov, and J. Schmalian, Adv. Phys. **52**, 119 (2003); A. V. Chubukov, D. Pines, and J. Schmalian, in *The Physics of Superconductors*, edited by K. H. Bennemann and J. B. Ketterson (Springer, Berlin, 2003), Vol. 1, p. 495.
²⁵A. Chubukov, A. Finkelstein, R. Haslinger, and D. Morr, Phys. Rev. Lett. **90**, 077002 (2003).
²⁶A. V. Chubukov, V. M. Galitski, and V. M. Yakovenko, Phys. Rev. Lett. **94**, 046404 (2005).
²⁷N. D. Mathur, F. M. Grosche, S. R. Julian, I. R. Walker, D. M. Freye, R. K. W. Haselwimmer, and G. G. Lonzarich, Nature (London) **394**, 39 (1998).
²⁸Y. Maeno, H. Hashimoto, K. Yoshida, S. Nishizaki, T. Fujita, J. G. Bednorz, and F. Lichtenberg, Nature (London) **372**, 532 (1994).
²⁹S. Saxena, P. Agarwal, K. Ahilan, F. Grosche, R. Haselwimmer, M. Steiner, E. Pugh, I. Walker, S. Julian, P. Monthoux, G. Lonzarich, A. Huxley, I. Sheikin, D. Braithwaite, and J. Flouquet, Nature (London) **394**, 39 (1998).
³⁰D. Aoki, A. Huxley, E. Ressouche, D. Braithwaite, J. Flouquet, J.-P. Brison, E. Lhotel, and C. Paulsen, Nature (London) **413**, 61 (2001).
³¹Z. Fisk and D. Pines, Nature (London) **394**, 22 (2001).
³²D. T. Son, Phys. Rev. D **59**, 094019 (1999).
³³D. J. Gross and F. Wilczek, Phys. Rev. Lett. **30**, 1343 (1973); H. D. Polizer, *ibid.* **30**, 1346 (1973).
³⁴D. Bailin and A. Love, Phys. Rep. **107**, 325 (1984).
³⁵M. Alford, K. Rajagopal, and F. Wilczek, Phys. Lett. B **422**, 247 (1998).
³⁶R. Rapp, T. Schafer, E. V. Shuryak, and M. Velkovsky, Phys. Rev.

- Lett. **81**, 53 (1998).
- ³⁷T. Schäfer and F. Wilczek, Phys. Rev. D **60**, 114033 (1999).
- ³⁸R. D. Pisarski and D. H. Rischke, Phys. Rev. D **61**, 051501(R) (2000).
- ³⁹The condition $g \ll 1$ near SDW or CDW instabilities can still be valid in some cases, but requires extra assumptions about the behavior of the interaction $u(r)$ in real space (Ref. 23).
- ⁴⁰T. Holstein, R. E. Norton, and P. Pincus, Phys. Rev. B **8**, 2649 (1973).
- ⁴¹M. Yu. Reizer, Phys. Rev. B **40**, 11571 (1989).
- ⁴²R. Pisarski and D. Rischke, Nucl. Phys. A **702**, 177 (2002).
- ⁴³J. Bardeen, L. N. Cooper, and J. R. Schrieffer, Phys. Rev. **108**, 1175 (1957).
- ⁴⁴C. M. Varma, P. B. Littlewood, S. Schmitt-Rink, E. Abrahams, and A. E. Ruckenstein, Phys. Rev. Lett. **63**, 1996 (1989).
- ⁴⁵P. B. Littlewood and C. M. Varma, Phys. Rev. B **46**, 405 (1992).
- ⁴⁶Q. Wang and D. H. Rischke, Phys. Rev. D **65**, 054005 (2002).
- ⁴⁷Physically, a finite Φ_0 can be realized by coupling our system to another superconductor through a weak Josephson junction.
- ⁴⁸P. B. Allen and R. C. Dynes, Phys. Rev. B **12**, 905 (1975).
- ⁴⁹J. P. Carbotte, Rev. Mod. Phys. **62**, 1027 (1990).
- ⁵⁰F. Marsiglio and J. P. Carbotte, Phys. Rev. B **33**, 6141 (1986).
- ⁵¹R. Combescot, Phys. Rev. B **51**, 11 625 (1995).
- ⁵²V. L. Pokrovski, JETP Lett. **47**, 629 (1988).
- ⁵³V. L. Emery and S. A. Kivelson, Nature (London) **374**, 434 (1995).
- ⁵⁴M. Franz and A. J. Millis, Phys. Rev. B **58**, 14 572 (1999); H. J. Kwon and A. T. Dorsey, *ibid.* **59**, 6438 (1999).
- ⁵⁵A. V. Chubukov, Phys. Rev. B **72**, 085113 (2005).
- ⁵⁶The restriction to Ising systems is important as the transition becomes otherwise of first order (Ref. 25).
- ⁵⁷P. W. Anderson, Science **235**, 1196 (1987).
- ⁵⁸C. Gross, R. Joynt, and T. M. Rice, Z. Phys. B: Condens. Matter **68**, 425 (1987); C. Gros, Phys. Rev. B **38**, 931 (1988).
- ⁵⁹A. Paramekanti, M. Randeria, and N. Trivedi, Phys. Rev. Lett. **87**, 217002 (2001); Phys. Rev. B **70**, 054504 (2004).
- ⁶⁰J. Liu, J. Schmalian, and N. Trivedi, Phys. Rev. Lett. **94**, 127003 (2005).
- ⁶¹This result is consistent with the experimental observation (Ref. 62) that T_c in underdoped cuprates scales with the neutron peak frequency. Note in this regard that in quantum-critical, exciton scenario of the neutron peak (Refs. 24 and 63) the resonance peak frequency is $\Omega_{\text{res}} \sim (\Delta \omega_{SF})^{1/2}$ where Δ is a gap, and ω_{SF} is the spin-fluctuation frequency. At strong coupling, $\Delta \sim \omega_{SF} \sim t^2/u \sim J$, and $\Omega_{\text{res}} = O(J)$.
- ⁶²H. F. Fong, B. Keimer, D. Reznik, D. L. Milius, and I. A. Aksay, Phys. Rev. B **54**, 6708 (1996); P. Dai, H. A. Mook, S. M. Hayden, G. Aeppli, T. G. Perring, D. Hunt, and F. Dogan, Science **284**, 1344 (1999); H. F. Fong, P. Bourges, Y. Sidis, L. P. Regnault, J. Bossy, A. Ivanov, D. L. Milius, I. A. Aksay, and B. Keimer, Phys. Rev. B **61**, 14773 (2000).
- ⁶³M. R. Norman and H. Ding, Phys. Rev. B **57**, R11 089 (1998); M. Eschrig and M. R. Norman, Phys. Rev. Lett. **85**, 3261 (2000).
- ⁶⁴A. J. Leggett, in *Modern Trends in the Theory of Condensed Matter*, edited by A. Pekalski and R. Przystawa (Springer-Verlag, Berlin, 1980).
- ⁶⁵P. Nozieres and S. Schmitt-Rink, J. Low Temp. Phys. **59**, 195 (1985).
- ⁶⁶R. T. Scalettar, E. Y. Loh, J. E. Gubernatis, A. Moreo, S. R. White, D. J. Scalapino, R. L. Sugar, and E. Dagotto, Phys. Rev. Lett. **62**, 1407 (1989).
- ⁶⁷C. A. R. Sa de Melo, M. Randeria, and J. R. Engelbrecht, Phys. Rev. Lett. **71**, 3202 (1993).
- ⁶⁸Ar. Abanov, B. L. Altshuler, A. Chubukov, and E. Yuzbashyan (unpublished).
- ⁶⁹D. V. Khveshchenko and W. F. Shively, cond-mat/0510519 (unpublished).